ISSN 2347 - 3983
Volume 11. No.3, March 2023
International Journal of Emerging Trends in Engineering Research
Available Online at http://www.warse.org/IJETER/static/pdf/file/ijeter021132023.pdf
https://doi.org/10.30534/ijeter/2023/021132023

# Limit analysis of masonry vaulted structures: the Santa Margherita Nuova Complex in Procida

**M. Candela[1], E. Liccardo[2], G. Riccardo[3], F. Tropeano[4]**
[1,2,3,4] University of Naples Federico II, Italy,
[1]ing.mcandela@libero.it,
[2]eugenio.liccardo@unina.it,
[3]gennaro.riccardo@unina.it,
[4] francesca.tropeano@unina.it

Received Date: January 27, 2023 Accepted Date: February 26, 2023 Published Date : March 07, 2023

## ABSTRACT

The paper aims to introduce some general concepts and issues about the complex operation of masonry vaulted structures. General setup is presented with formulas for analytical treatment, and checks about current operative and collapse conditions. Concepts are later used to verify the functioning of a vaulted structure embedded in the monumental Santa Margherita Nuova complex in Procida using FEM analyses.

**Key words :** Masonry structures, Vaulted constructions, historical and monumental heritage, collapse prevention.

## 1. INTRODUCTION

Vaulted masonry structures began to spread as early as the 3rd millennium B.C. in Egypt and Mesopotamia. The use and knowledge of this structural type made it possible to replace the trilithic system with the ability to cover larger spans. Masonry bases its structural efficiency on the compressive strength which turns into the axial forces' transmission –between elements. Masonry vaults deviate from the trilithic system in that they do not exert a vertical action on the piers but a thrust capable of flipping the entire structure.
In the following the general approach to the treatment of masonry structures is outlined, giving some synthetic insights on the masonry material behaviour with its admissibility conditions, and approaches for checks about fracture and failure, collapse activation by briefly recalling the limit analysis theorems for masonry. Thereafter the monumental site that is referred to, the Santa Margherita Nuova in Procida, is referred to in Sect.2, and the results from a numerical FEM campaign are shortly reported.

## 1. LIMIT ANALYSIS EXTENDED TO NON-TENSILE RESISTANT SOLIDS

To apply limit analysis as a method of analysis for masonry arches and vaults, one may take advantage of the assumptions introduced by Heyman (see [1]-[4]) about the behaviour of these structures:

a) The masonry has no tensile strength: although the stone has a definite tensile strength, the joints between ashlars can be made with weak mortar or be dry.
b) The ashlars cannot slip relative to each other: therefore, it is assumed that the friction between ashlars is high enough to prevent them from slipping. This means assuming that the shear component exerted between two contiguous ashlars does not exceed the friction force.
c) Masonry has infinite compressive strength: this means assuming that the stresses are so low that they do not cause crushing of the material. Although this is an unsafe assumption it turns out to be well verified, since under normal operating conditions the average stresses are always lower than the limiting stresses.

### 1.1 Admissibility conditions

From these assumptions it is possible to derive the admissibility conditions Eq.(1) imposed by the NT (non-tensile resistant) material according to which a generic admissible stress state $\boldsymbol{\sigma}$ cannot perform positive work for the generic fracture-strain $\boldsymbol{\varepsilon}_f$:

$$\boldsymbol{\sigma} \cdot \boldsymbol{\varepsilon}_f \leq 0 \qquad \forall\, \boldsymbol{\sigma} \in D_0 \tag{1}$$

where the generic stress state is defined as purely compressive $\boldsymbol{\sigma} \leq \mathbf{0}$, since zero tensile strength of the material is assumed. The generic allowable fracture strain range is defined as semi-positive at every point of the solid $\boldsymbol{\varepsilon}_f \geq \mathbf{0}$, since under these assumptions the only possible failure mechanism is the formation of opening hinges by relative rotation of the ashlars, thus excluding interpenetration between ashlars, which is obviously unrealistic [5]-[11]. Thus, at hinges unilateral conditions are imposed on the sign of the rotations: extradox hinges correspond to a relative counterclockwise rotation and are therefore defined as positive, while intradossal hinges correspond to a relative clockwise rotation.

### 1.2 Collapse condition

In masonry structures one assumes that no energy dissipation occurs when developing fractures (for some references see [12]- [29], also with reference to protection, refurbishment and dynamic control [30]-[47]); masonry structures are still able to maintain their strength during the development of the collapse mechanism

$$\boldsymbol{\sigma} \square \boldsymbol{\varepsilon_f} = 0 \tag{2}$$

Let analyze a masonry structure subject to surface forces **p** acting on the free surface $S_p$ and volume forces **F** acting in the volume V. It is possible to decompose the loads into a fixed rate ($\overline{\boldsymbol{p}}$ , $\overline{\boldsymbol{F}}$) and a variable rate ($\lambda\widehat{\boldsymbol{p}}$, $\lambda\widehat{\boldsymbol{F}}$) dependent therefore on the value of the load multiplier λ. One assumes that the structure is stable subjected only to fixed loads, and therefore only variable loads can make the structure unstable.

One has the following conditions:

a) Equilibrium: equilibrium between internal forces and external loads is guaranteed if

$$\int_V \boldsymbol{\sigma} \cdot \boldsymbol{\varepsilon}\, dV = \int_{S_p} (\overline{\boldsymbol{p}} + \lambda\widehat{\boldsymbol{p}})\, \boldsymbol{u}\, ds + \int_V \left(\overline{\boldsymbol{F}} + \lambda\widehat{\boldsymbol{F}}\right) \boldsymbol{u}\, dV$$
$$\forall\, \boldsymbol{u}\,,\ \boldsymbol{\varepsilon} = \Delta \boldsymbol{u} \tag{3}$$

b) Mechanism: enough hinges are introduced to allow for kinematics, and they are activated in precise ways. The mechanism is a collapse mechanism $\mathbf{u}_c$ under the assigned loads if

$$\int_{S_p} (\overline{\boldsymbol{p}} + \lambda\widehat{\boldsymbol{p}}) \cdot \boldsymbol{u}_c\, ds + \int_V \left(\overline{\boldsymbol{F}} + \lambda\widehat{\boldsymbol{F}}\right) \cdot \boldsymbol{u}_c\, dV > 0 \tag{4}$$

c) Admissibility: a stress respectful of the material limit strength and complying with masonry admissibility (pure compression/null stress) must be verified at each point of the solid. Fracture strains also have to comply with strain admissibility, whence

$$\boldsymbol{\sigma} \cdot \boldsymbol{\varepsilon} \leq 0 \tag{5}$$

d) Variable loads: the work done by variable loads during the activation of the $\mathbf{u}_c$ collapse mechanism is positive.

$$\int_{S_p} \widehat{\boldsymbol{p}} \square \boldsymbol{u_c}\, ds > 0, \int_V \widehat{\boldsymbol{F}} \square \boldsymbol{u}_c\, dV > 0 \tag{6}$$

### 1.3 Fundamental theorems of limit analysis

The proportional rise of loads may be considered according to the load multiplier λ. Thus, the problem is reduced to the identification of this parameter at the collapse condition. To this aim, it is possible to take advantage of the two fundamental theorems of limit analysis: the Static Theorem and the Kinematic Theorem.

To summarize, the two fundamental theorems of limit analysis for NRT solids make it possible to identify the load multiplier $\lambda_c$ with which a collapse mechanism is associated, and which therefore limits the load-bearing capacity of the structure. According to the static theorem, the collapse load multiplier $\lambda_c$ corresponds to the maximum of the statically admissible multipliers $\lambda_s$.
The Kinematic Theorem identifies the minimum of the kinematically sufficient multipliers $\lambda_k$ as the collapse load multiplier $\lambda_c$.
In this way, the two limit analysis theorems make it possible to define two load multipliers, $\lambda_s$ and $\lambda_k$, which constitute a minor and a major of the collapse load multiplier $\lambda_c$, respectively

$$\max\{\lambda_s\} \ \leq\ \lambda_c \ \leq\ \min\{\lambda_k\} \tag{7}$$

## 2. SANTA MARGHERITA NUOVA COMPLEX

The complex of Santa Margherita Nuova dates back to the 15th century and was built to house Dominican monks who had abandoned the Cenobio of Santa Margherita. The underlying soil underwent severe morphological disintegration, which over the centuries led to the underlying rocky isthmus crumbling to the point of causing major damage (Figure 1) to the complex in 1956, due to several collapses.

**Figure 1:** South-est and south-west fronts**.**

To cope with this situation, several interventions were implemented to consolidate and restore the structure, particularly the reconstruction of the imponent vaults placed to support the complex on the southwest front.
For the reconstruction of the structure, tuff quarries located in the immediate vicinity of the intervention area were searched with the aim of preserving the rheological characteristics of the existing structure. The masonry obtained, with the use of M15 guaranteed performance mortar, has characteristics almost similar to the existing masonry.

The values of the mechanical characteristics of the existing masonry were obtained by conducting some tests executed on the complex that allowed the material to be classified.
Below two tables are reported in Figure 2 with the main mechanical characteristics of the two masonries, showing that they have the same unit weight.

| | |
|---|---|
| **Moduli elastici** | |
| E | 3500 |
| G | 1400 |
| **Resistenze** | |
| f,k | 3.500 |
| f,tm | 0.000 |
| f,hk | 2.650 |
| τ,0 | |
| f,vk0 | 0.200 |
| **Altre proprietà meccaniche** | |
| w | 16.00 |
| α | 0.000010 |
| f,b | 10.000 |
| μ | 0.577 |
| φ | 1.000 |
| **Blocchi e malta** | |
| f,bk | 5 |
| f',bk | 2.5 |
| fm,m | 15 |

(a)

| | |
|---|---|
| **Moduli elastici** | |
| Valori | Medi |
| E | 1410 |
| G | 450 |
| **Resistenze** | |
| Valori | Medi |
| f,m | 2.600 |
| f,tm | 0.260 |
| f,hm | 1.300 |
| τ,0 | 0.060 |
| f,vm0 | 0.145 |
| **Altre proprietà meccaniche** | |
| w | 16.00 |
| α | 0.000010 |
| f,b | 10.000 |
| μ | 0.577 |
| φ | 1.000 |

(b)

**Figure 2:** Mechanical characteristics of new masonry made of regular soft stone ashlars, Neapolitan yellow tuff (a) and characteristics of existing masonry made of regular soft stone ashlars (b).

### 2.1 FEM analysis

In the following some FEM analyses are executed for evaluating the stress distribution within the structure by identifying under different loading conditions where the greatest tensile stresses are expected to occur at least in an indicative form. This is because areas where tensile stresses occur are prone to cracking.
The numerical tests are executed for the two cases (ante or post reconstruction), starting from the analyses under self-weight. Then two different loading conditions were considered. The first consists of a vertical distributed load of $6 \cdot E^4$ KN/m$^2$ applied on the first two arches while the second consists of a concentrated horizontal force of $6 \cdot E^4$ KN applied at the top of the structure.
To evaluate the stress distribution, it was considered that in each resisting section there is a bilinear type of stress distribution starting from the minimum compression $\sigma_{min}$ to the opposite maximum stresses $\sigma_{max}$.
Both values are represented by means of a graphic scale with intensities expressed in KN/m$^2$.
The two models subjected to self-weight have similar behaviors. From the observation of the deformations (Figure 3) what is evident is a sagging of the first two arches that is more pronounced in comparison with the other arch.
From the distribution of stresses, values of $\sigma_{min}$ of pure compression are recorded that increase as one goes down inside the piers, recording maximum values at the foot of the piers. For the distribution of $\sigma_{max}$, however, lower compressive values are recorded, but these values, although low, turn out to be tensile near the keystone section.

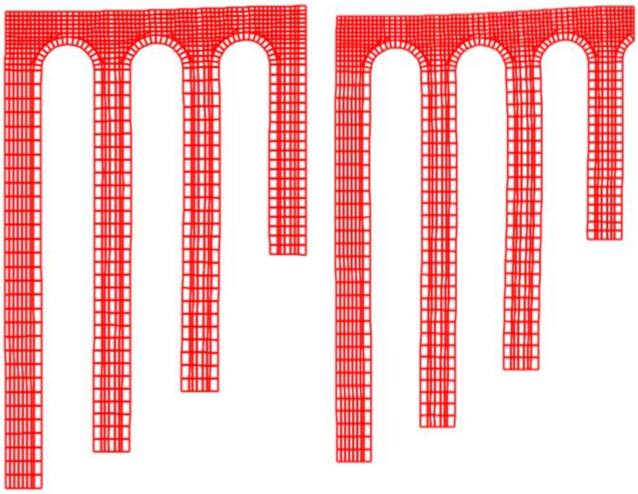

(a) (b)
**Figure 3:** Deformation of the restored structure (a) and the original structure (b) subjected to the self-weight.

For the first loading condition, both the original and the reconstituted structure show deformations very similar to those related to self-weight alone, with a more pronounced sagging of the two arches affected by the distributed load with consequent horizontal displacement of the corresponding piers as well.
For the new structure, minimum pure compressive stress values are observed throughout, with lower values near the arches and higher values near the foot of the piers. For maximum tension values (Figure 4 for the reconstructed structure and Figure 5 for the original one), however, pure compressive values are recorded throughout the structure except for the two arches affected by the distributed load. In these two arches, although low, tensile values can be detected near the keystone section.
A similar situation occurs for the original structure, where, however, the compressive values are found to be higher in the last pier as compared to the restored structure.

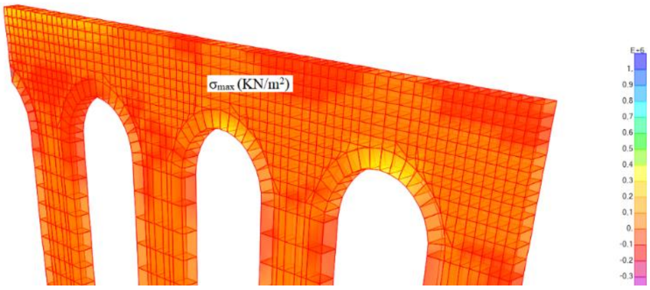


**Figure 4:** Distribution of $\sigma_{max}$ (KN/m$^2$) in details on the arches of the reconstructed structure subjected to a vertical distributed load ($6 \cdot E^4$ KN/m$^2$) (3D view).

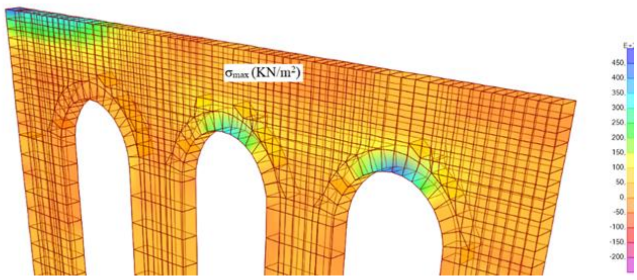


**Figure 5:** Distribution of $\sigma_{max}$ (KN/m$^2$) in details on the arches of the original structure subjected to a vertical distributed load ($6 \cdot E^4$ KN/m$^2$) (3D view).

In comparison with the new structure, higher tensile values are observed in the original structure in the arches near the keystone section.

For the load corresponding to a horizontal force applied at the top, in both structures it causes a shift in the direction of the force of the entire upper part of the structure resulting in the lowering of the first two arches.

The structures return a response in terms of stresses very close to each other. A pure compressive $\sigma_{min}$ distribution is recorded, reaching maximum values at the foot of the piers and minimum values at the top. For the distribution of $\sigma_{max}$ (Figure 6 and Figure 7), it can be seen that very low tensile values are recorded, practically close to zero, except for the shutters of the arches where, on the other hand, compressive values are also read for $\sigma_{max}$.

## 3. CONCLUSIONS

In the paper one deals with historical masonry construction, an in particular with a monumental complex in the island of Procida, close to Naples, that experienced some partial failure. Numerical analyses performed on the original and on the restored structure allow to compare date and relate the collapse to the morphological disintegration of the underlying soil.

The reconstructed structure exhibits a behavior similar to the original one. The substantial difference is evident in the last right pier of the multiple arched supporting structure, where, due to the thrust of the additional arcade introduced in the restored structure, the stress values turn out to be lower.

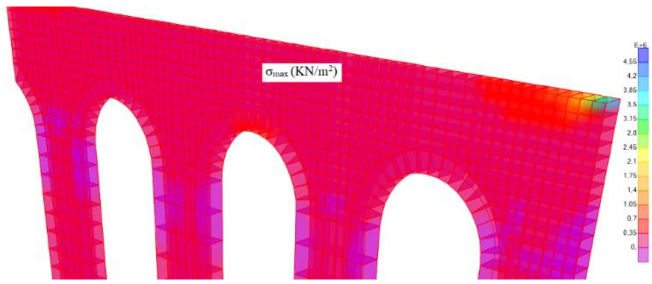


**Figure 6:** Distribution of $\sigma_{max}$ (KN/m$^2$) in detail on the arches of the reconstructed structure subjected to a horizontal force applied at the top ($6 \cdot E^4$ KN) (3D View).

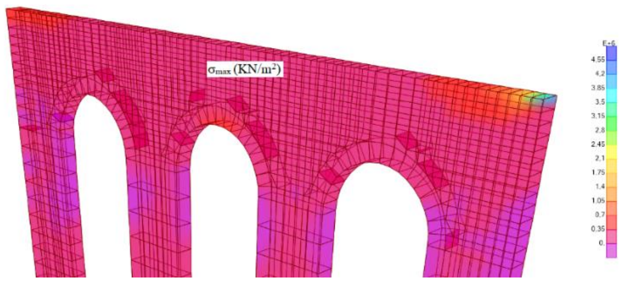


**Figure 7:** Distribution of $\sigma_{max}$ (KN/m$^2$) in detail on the arches of the original structure subjected to a horizontal force applied at the top ($6 \cdot E^4$ KN) (3D View)

## REFERENCES


[1] Heyman J., **The stone skeleton**. J. of Solids and Structures. Vol.2, 269-279, 1996.

[2] Heyman, J. ***Equilibrium of shell structures,*** Oxford University Press, 1977.

[3] Heyman J. ***The masonry arch.*** Cambridge press, Cambridge, 1982.

[4] Heyman J. ***Poleni's problem***. University of Cambridge, 1988

[5] Heyman J. ***The stone skeleton.*** Cambridge Univ. Press, 1997.

[6] Baratta, A., Corbi, O. **An approach to the positioning of FRP provisions in vaulted masonry structures**, J. Composites Part B: Engineering, vol. 53, 334 – 341, doi: 10.1016/j.compositesb.2013.04.043, ISSN: 13598368 (2013).

[7] Baratta, A., Corbi, O. **Stress Analysis of Masonry Vaults and Static Efficacy of FRP Repairs**, Intern. Journal of Solids and Structures, vol.44(24), 8028-8056. ISSN: 0020-7683 (2007).

[8] Baratta, A., Corbi, O. **On Variational Approaches in NRT Continua**. Intern. Journal of Solids and Structures, 42, 5307-5321, Int. J. Solids and Structures, ISSN: 0020-7683 (2005).

[9] Baratta, A., Corbi, I. **Topology optimization for reinforcement of no-tension structures**, J.Acta Mechanica, 225, pp. 663-678 (2014).

[10] Baratta, A., Corbi, O. **Relationships of L.A. Theorems for NRT Structures by Means of Duality**, Intern.

Journal of Theoretical and Applied Fracture Mechanics, 44, 261-274 (2005).

[11]Baratta, A., Corbi, O. **Duality in Non-Linear Programming for Limit Analysis of NRT Bodies**. Int. J. Structural Engineering and Mechanics, 26(1), 15-30 (2007).

[12]Baratta, A., Corbi, I., Corbi, O.,D.Rinaldis, **Experimental Survey on Seismic Response of Masonry Models**. In "Structural Analysis of Historic Constructions: Preserving Safety and Significance". D' Ayala and E. Fodde Eds. Balkema Book, CRC Press:799-806 (2008).

[13]Baratta, A., Corbi, I., Corbi, O. **Stress Analysis of Masonry Structures: Arches, Walls, and Vaults**. In "Structural Analysis of Historic Constructions: Preserving Safety and Significance". D'Ayala and E. Fodde Eds. Balkema Book, CRC Press: 321-329 (2008).

[14]Baratta, A., Corbi, O. **On the equilibrium and admissibility coupling in NT vaults of general shape**, Int J Solids and Structures, vol.47(17), 2276-2284 (2010).

[15]Baratta, A., Corbi, O. **The treatment of masonry vaults through the Monge-Ampère equation**, Int J Mathematical Models and Methods in Applied Sciences, vol.7 (10), 854 – 862 (2013).

[16]Baratta, A., Corbi, O. **Contribution of the fill to the static behaviour of arched masonry structures: Theoretical formulation**, J.Acta Mechanica, vol.225 (1), 53 – 66, (2014).

[17]Baratta, A., Corbi, O. **Closed-form solutions for FRP strengthening of masonry vaults, J. Computers and Structures**, vol.147, pp.244-249 (2015).

[18]Baratta, A., Corbi, I., Corbi, O. **Analytical Formulation of Generalized Incremental Theorems for 2D No-Tension Solids**, J. Acta Mechanica, vol.226(9), pp.2849-2859 (2015).

[19]Baratta, A., Corbi, I., Corbi, O. **Stability of evolutionary brittle-tension 2D solids with heterogeneous resistance**, J. Computers and Structures, vol.174, pp.133-138 (2016).

[20]Baratta, A., Corbi, O. **Heterogeneously Resistant Elastic-Brittle Solids under Multi-Axial Stress: Fundamental Postulates and Bounding Theorems**, J. Acta Mechanica, vol.226(6), pp.2077-2087 (2015).

[21]Baratta, A., Corbi, I., Corbi, O. , **Bounds on the Elastic Brittle solution in bodies reinforced with FRP/FRCM composite provisions**, J. Composites Part B: Engineering, vol.68, 230-236 (2015).

[22]Corbi, I. **FRP Composites Retrofitting for Protection of Monumental and Ancient Constructions**, Open Construction and Building Technology Journal, vol.6, 361-367 (2012).

[23]Corbi, I. **FRP reinforcement of masonry panels by means of c-fiber strips**, J. Composites Part B, vol.47, 348-356 (2013).

[24]Corbi, I., Corbi, O. **Analysis of bi-dimensional solids with internal unilateral constraint coupled to structural elements with different degree of connection**, J. Acta Mechanica, vol.228(2), pp.607-616 (2017).

[25]Corbi, I., Corbi, O. **Theorems for masonry solids with brittle time-decaying tensile limit strength**, J. Acta Mechanica, vol. 228(3), pp.837-849 (2017).

[26]Corbi, I., Corbi, O. **Combinational optimization for shaping discrete tensile boost elements in continuum structures**, Acta Mechanica, vol.229(9), p.3575 (2018).

[27]Corbi, I., Corbi, O., F. Tropeano, **Stability assessment of an historical masonry bridge through the LA kinematic theorem for NT structures**, Int. J. Mechanics, vol.10, 305-311 (2016).

[28] Corbi, I., Corbi, O., Tropeano, F. **Analysis of the spatial behaviour of masonry bridges via hierarchical fem modelling: The Devil's bridge**, International Journal of Mechanics, vol.14, 72-78, (2020).

[29]Corbi, I., Corbi, O., Li, H. **Holonomic non-linear modelling for the analysis of heterogeneously resisting structures**, J. Engineering Solid Mechanics, vol.6(3), pp. 253-262 (2018).

[30]Corbi, O. **Optimal Distribution of Linear Control Intensity over the Frequency Range.** Intern. Journal of Earthquake Engineering and Structural Dynamics, Wiley & Sons. vol.32(2), 173-185. ISSN: 0098-8847. doi:10.1002/eqe211 (2003).

[31]Baratta, A., Corbi, O. **On the Dynamic Behaviour of Elastic-Plastic Structures Equipped with Pseudoelastic SMA Reinforcements.** Intern. Journal of Computational Materials Science, Elsevier Science. vol. 25(1-2), 1-13. ISSN: 0927-0256. doi:10.1016/S0927-0256(02)00245-8 (2002).

[32]O.Corbi. **Shape Memory Alloys and Their Application in Structural Oscillations Attenuation**, Intern. Journal of Simulation Modeling Practice and Theory (SIMPAT), vol.11, 387-402. ISSN: 1569-190X. doi:10.1016/S1569-190X(03)00057-1 (2003).

[33]Baratta, A., Corbi, O., **Dynamic Response and Control of Hysteretic Structures**, Intern. Journal of Simulation Modeling Practice and Theory (SIMPAT), vol.11, 371-385 (2003).

[34]Baratta, A., Corbi, O., Corbi, I. **Rocking Motion of Rigid Blocks and their Coupling with Tuned Sloshing Dampers**. In B.H.V. Topping, L.F. Costa Neves and R.C. Barros (eds.), CC09, Proc. 12th Intern. Conf. on Civil, Structural and Environmental Engineering Computing., Civil Comp-Press, Stirlingshire, UK. Paper 175. Madeira, Portugal, 1-4 September (2009).

[35]Li, H., Hong, C., Xiong, Z., Lorenzo R., Corbi, I., Corbi, O. **Experimental investigation on axial compression behavior of laminated bamboo lumber short columns confined with CFRP**. J.Composites Part A: Applied Science and Manufacturing, vol.150, 106605, doi: 10.1016/j.compositesa.2021.106605 (2021)

[36]Yang, D., Li, H.,Xiong, Z., Mimendi, L., Lorenzo, R., Corbi, I., Corbi, O., Hong, C. **Mechanical Properties of Laminated Bamboo Under Off-axis Compression**, Composites Part A, 2020, vol. 138, 106042, doi: 10.1016/j.compositesa.2020.106042

[37]Li, H., Qiu, Z.,Wu, Corbi, O., G., Wei, D. ,Wang, L., Corbi, I.,Yuan, C. **Slenderness Ratio Effect on Eccentric Compression Properties of Parallel Bamboo Strand Lumber Columns,** J. Structural Engineering, vol.145(8), 04019077, doi: 10.1061/(ASCE)ST.1943-541X.0002372 (2019).

[38]Baratta, A., Corbi, I., Corbi, O. **Algorithm design of an hybrid system embedding influence of soil for dynamic vibration control**, J. Soil Dynamics and Earthquake Engineering, vol.74, 79-88, (2015)

[39]Baratta, A., Corbi, I., Corbi, O., Mastorakis, N. **Strategies for the protection from structural failures under seismic events**, International Journal of Mechanics, vol.9, 69-75 (2015).

[40]Corbi, O., Zaghw, A.H. **Properties and design of dissipative viscorecentring SMA members for civil structures**, Int. J. Mechanics, vol.7(3), .285 – 292, (2013).

[41]Corbi, O., Zaghw, A.H., Elattar, A., Saleh, A. **Preservation provisions for the environmental protection of egyptian monuments subject to structural vibrations**, Int. J. Mechanics, vol.7(3), 172 – 179, (2013).

[42]Corbi, I., Corbi, O. **Macro-mechanical modelling of pseudo-elasticity in shape memory alloys for structural applications**, J. Acta Mechanica, vol.227(8), 2171-2179, (2016).

[43]Corbi, I., Corbi, O., Li, H. **Optimum design of dynamic modal control algorithm using non-linear structural mathematical modelling** , J. Soil Dynamics and Earthquake Engineering, vol.114, pp.548-554, (2018).

[44]Corbi, I., Corbi, O. **Development and implementation of a control system for the dynamic mitigation of 3-D masonry structures with feedback on the drifts in the horizontal plane**, J. Structural Control and Health Monitoring, vol.25(8), 1-12, (2018).

[45]Corbi, I., Corbi, O., Li, H. **A Constrained Energy Minimum Approach to Modal Dynamic Control of Vibrations in Ancient Nonlinear Structures**, Int. Journal of Structural Stability and Dynamics, vol.19(6),1950054, (2019).

[46]Corbi, I., Corbi, O., Li, H. **A coupled control strategy for the mitigation of structural vibrations**, Ingegneria Sismica, vol.36(3), 107-117 (2019).

[47]Corbi, I., Corbi, O., Li, H. **Convolutive PD controller for hybrid improvement of dynamic structural systems**. J. Soil Dynamics and Earthquake Engineering, vol.137, 106255, (2020).